Systems analysis of the neuroinflammatory and hemodynamic response to traumatic brain injury

Rowan O. Brothers[#1],

Sara Bitarafan[#2,3],

Alyssa F. Pybus[1,3],

Levi B. Wood[1,2,3,¥,^],

Erin M. Buckley[1,4,5,¥,^]

[1]Wallace H. Coulter Department of Biomedical Engineering, Georgia Institute of Technology and Emory University, USA

[2]George W. Woodruff School of Mechanical Engineering, Georgia Institute of Technology, USA

[3]Parker H. Petit Institute for Bioengineering and Bioscience, Georgia Institute of Technology, USA

[4]Department of Pediatrics, Emory University School of Medicine, USA

[5]Children's Healthcare of Atlanta, Children's Research Scholar, USA

[#] These authors contributed equally to this work.

Abstract

Mild traumatic brain injuries (mTBIs) are a significant public health problem. Repeated exposure to mTBI can lead to cumulative, long-lasting functional deficits. Numerous studies by our group and others have shown that mTBI stimulates cytokine expression and activates microglia, decreases cerebral blood flow and metabolism, and impairs cerebrovascular reactivity. Moreover, several works have reported an association between derangements in these neuroinflammatory and hemodynamic markers and cognitive impairments. Herein we detail methods to characterize the neuroinflammatory and hemodynamic tissue response to mTBI in mice. Specifically, we describe how to perform a weight-drop model of mTBI, how to longitudinally measure cerebral blood flow using a non-invasive optical technique called Diffuse Correlation Spectroscopy, and how to perform a Luminex multiplexed immunoassay on brain tissue samples to quantify cytokines and immunomodulatory phospho-proteins (e.g., within the MAPK and NFκB pathways) that respond to and regulate activity of microglia and other neural immune cells. Finally, we detail how to integrate these data using a multivariate systems analysis approach to understand the relationships between all of these variables. Understanding the relationships between these physiologic and molecular variables will ultimately enable us to identify mechanisms responsible for mTBI.

DISCLOSURES
None.

SUMMARY:

This protocol presents methods to characterize the neuroinflammatory and hemodynamic response to mild traumatic brain injury and to integrate these data as part of a multivariate systems analysis using partial least squares regression.

Keywords

Mild traumatic brain injury; cerebral blood flow; neuroinflammation; multiplexed ELISA; partial least squares regression; cytokines; phospho-proteins

INTRODUCTION

Overview

Mild traumatic brain injuries (mTBIs) impact ~1.6–3.8 million athletes annually[1]. These injuries, including sub-concussive and concussive injuries, can leave patients with transient physical, emotional, psychological and cognitive symptoms[2]. Moreover, *repetitive* mTBI (rmTBI) sustained within a "window of vulnerability" can lead to cumulative severity and duration of cognitive consequences that last longer than the effects of a single mTBI alone[3], and ultimately even to permanent loss of function[4–6]. Although many patients recover within a relatively short time frame (<1 week), 10–40% of patients suffer longer lasting effects of mTBI for > 1 month, with some lasting up to 1 year[3, 7–9]. Despite the high prevalence and lasting consequences of these injuries, injury mechanisms are poorly understood and no effective treatment strategies exist.

Given the high variability in outcomes after mTBI/rmTBI, one challenge in identifying early-stage molecular triggers from tissue obtained in terminal mTBI/rmTBI studies is the lack of longitudinal data demonstrating definitive acute links to longer-term outcomes. To overcome this challenge, our group has discovered that acutely reduced cerebral blood flow, measured acutely using an optical tool called diffuse correlation spectroscopy (DCS), strongly correlates with longer-term cognitive outcome in a mouse model of rmTBI [10]. Using this hemodynamic biomarker, we showed that mice with acutely low cerebral blood flow (and, by extension, worse predicted long-term outcome) have concomitant acute increases in neuronal phospho-signaling within both MAPK and NFκB pathways, increases in neuronal expression of pro-inflammatory cytokines, and increases in expression of the phagocyte/microglial marker Iba1[11]. These data suggest a possible role for neuronal phospho-signaling, cytokine expression, and microglial activation in both the acute regulation of cerebral blood flow post injury as well as in triggering a signaling cascade that leads to neuronal dysfunction and worse cognitive outcome. Herein, we detail our approach to simultaneously probe both the hemodynamic and neuroinflammatory environment after rmTBI and how to integrate these complex datasets. Specifically, we outline procedures for four key steps to this comprehensive approach: (1) A weight-drop model of mild traumatic brain injury, (2) Assessment of cerebral blood flow with Diffuse Correlation Spectroscopy, (3) Quantification of the neuroinflammatory environment, and (4) Data integration (Fig. 1). Below we provide a brief introduction to each of these key steps to help guide our

readers through the rationale behind our methods. The remainder of the manuscript provides a detailed protocol for each of these key steps.

Weight-Drop Model of Mild Traumatic Brain Injury

Although many excellent preclinical models of repetitive mild TBI exist[12–18], we employ a well-established and clinically relevant weight-drop closed head injury model. Key features of this model include (1) blunt impact of the intact skull/scalp followed by unrestricted rotation of the head about the neck, (2) no overt structural brain injury, edema, blood–brain barrier damage, acute cell death, or chronic brain tissue loss, and (3) persistent (up to 1 year) cognitive deficits that emerge only after multiple hits[19] (Fig. 2).

Assessment of Cerebral Blood Flow with Diffuse Correlation Spectroscopy

Diffuse correlation spectroscopy (DCS) is a non-invasive optical technique that measures blood flow [5, 20, 21]. In DCS, a near-infrared light source is placed on the tissue surface. A detector is placed at a fixed distance from the source on the tissue surface to detect light that has multiply-scattered through the tissue (Fig. 3). Scattering off moving red blood cells causes the detected light intensity to fluctuate with time. A simple analytical model known as correlation diffusion theory is used to relate these intensity fluctuations to an index of blood flow (CBF_i, Fig. 4). Although the units of CBF_i (cm^2/s) are not the traditional units of flow (mL/min/100 g), a previous study in mice has shown that CBF_i strongly correlates with cerebral blood flow measured by arterial spin labeled MRI[21].

For reference, our DCS instrument was built in-house and is comprised of an 852 nm long coherence-length laser, an array of 4 photon counting avalanche photodiodes, and a hardware autocorrelator board (multi-tau, 8 channel, 100 ns minimum sample time)[21, 22]. Data is acquired with homemade software written in LabView. The animal interface for the device consists of a 400 μm multimode source fiber (400–2200 nm wavelength range, pure silica core, TECS Hard Cladding) and a 780 nm single mode detector fiber (780–970 nm wavelength range, pure silica core, TECS Hard Cladding, 730 +/− 30 nm second mode cut-off) spaced 6 mm apart and embedded in a black 3D-printed sensor (4 mm × 8 mm, seen in Fig. 3).

Quantification of the Neuroinflammatory Environment

Although neuroinflammation is regulated by diverse cellular processes, two key relevant mechanisms are extracellular signaling by cytokines/chemokines and intracellular signaling by phospho-proteins. To investigate the neuroinflammatory environment of the brain post-injury, brains are extracted from mice, microdissected, and cytokines/chemokines and phospho-proteins are quantified using Luminex (Fig. 5, 6, and 7). Luminex multiplexed immunoassays enable simultaneous quantification of a diverse collection of these proteins by coupling enzyme-linked immunosorbent assays (ELISAs) to fluorescently tagged magnetic beads. Distinct fluorescent tags are used for each protein of interest, and beads of each tag are functionalized with a capture antibody against that particular protein. Hundreds of beads for capturing each protein are mixed together, placed in a 96 well plate, and incubated with sample. After sample incubation, a magnet is used to trap the beads in the well while the sample is washed out. Next, biotinylated detection antibody

binds to the analyte of interest to form an antibody-antigen sandwich similar to a traditional ELISA, but with the ELISA for each protein occurring on a different fluorescently tagged bead. Adding phycoerythrin-conjugated streptavidin (SAPE) completes each reaction. The Luminex instrument then reads the beads and separates the signal according to each fluorescent tag/protein.

Data Integration

Because of the large number of analytes (e.g., cytokines) measured in the Luminex assay, data analysis can be difficult to interpret if each quantified protein is analyzed individually. To simplify analysis and to capture trends observed among analytes, we use a multivariate analysis method called partial least squares regression (PLSR, Fig. 8)[23]. PLSR works by identifying an axis of weights corresponding to each measured protein (i.e., cytokines or phospho-proteins, referred to as "predictor variables") that together optimally explain co-variance of the measured proteins with a response variable (e.g., cerebral blood flow). The weights are referred to as "loadings" and are assembled into a vector known as a latent variable (LV). By projecting (referred to as "scoring") the measured protein data on each of two LVs, the data can be re-plotted in terms of these LVs. After computing the PLSR, we use a varimax rotation to identify a new LV that maximizes the covariance between the sample projections onto the LV and the predictor variable[24]. This approach allows us to define LV1 as the axis for which the variance of the response variable is best explained. LV2 maximizes co-variance between the response variable and LV1 residual data, which may be associated with biological or technical variability between samples. Lastly, we conduct a Leave One Out Cross Validation (LOOCV) to ensure that the PLSR model is not heavily dependent upon any one sample[23].

PROTOCOL

All animal procedures are approved by Emory University Institutional Animal Care and Use Committee (IACUC) and followed the NIH Guidelines for the Care and Use of Laboratory Animals.

1.   Weight-drop Model of Mild Traumatic Brain Injury

1.1   Prepare weight-drop setup: Mount a vise on a flat surface with a 1 m guide tube (2.54 cm inner diameter) aligned vertically (check using a level). Use a 54 g bolt (0.95 cm basic body diameter, 2 cm head diameter, 10.2 cm length) for the impact.

1.2   Briefly anesthetize mouse: Induce mouse with 4.5% isoflurane in 100% oxygen for 45 seconds. Confirm sufficient depth of anesthesia by the lack of a toe pinch response.

1.3   Induce injury—1.3.1 Rapidly remove mouse from anesthesia, and place mouse prone on the center of a thin membrane (11.2×21.3 cm tissue).

1.3.2 Use both hands to hold the tissue taut with the mouse prone on the center. Secure the mouse's tail under your thumb. Position mouse head under the guide tube (Fig. 2).

1.3.3 Drop the bolt from the top of the guide tube onto the dorsal aspect of the mouse's head, aiming for impact between the back of the eyes and the front of the ears.

1.3.4 Upon impact, the mouse will penetrate the tissue, allowing for rapid acceleration of the head about the neck (Fig. 2).

1.4 Recovery: After impact, place mouse supine on a 37 °C warming pad in room air. Monitor recovery for 1 hr post-injury. Within 1hr, mice should be able to ambulate normally, find food and water, and not exhibit gross motor deficits.

NOTE: Loss of consciousness, defined as the time from removal from anesthesia to the time to regain righting reflex, is expected and typically lasts from 20 s to 3 minutes (Supplemental Table 1). Brief (<30 s) episodes of apnea and/or seizure-like activity may be observed, particularly after repetitive head injuries spaced once-daily.

1.5 Repeat as needed: This injury may be repeated once-daily, weekly, or monthly. The number and spacing of injuries depend on desired injury severity. Typically, our group employs five hits spaced once-daily to induce robust deficits in spatial learning and memory.

2. Assessment of Cerebral Blood Flow with Diffuse Correlation Spectroscopy

2.1 DCS data acquisition—2.1.1 Remove hair on scalp: Because DCS works best in the absence of hair, it is necessary to remove fur on the head prior to the start of experiments. Typically, hair removal is done 1–3 days prior to the start of the study.

2.1.1.1 Induce mice with 4.5% isoflurane in 100% oxygen for 45 seconds, and maintain with 1–2% isoflurane in 100% oxygen.

2.1.1.2 Shave the head between the eyes and the ears. Then, use depilatory cream to remove fur on the head as in Fig. 3.

2.1.1.3 Allow the animal to recover from anesthesia on a warming pad and then return to cage.

2.1.2 Measure cerebral blood flow with DCS: To minimize motion artifacts during measurement, mice are studied under brief isoflurane anesthesia.

NOTE: Visually monitor respiration and toe pinch response throughout measurements and adjust isoflurane concentration as needed to ensure consistent depth of anesthesia. Significant variations in the depth of anesthesia could alter blood flow given the known vasomodulatory effects of isoflurane[25].

2.1.2.1 Induce with 4.5% isoflurane in 100% oxygen for 45 seconds, and then maintain with 1.0–1.75% isoflurane in 100% oxygen. Confirm sufficient depth of anesthesia by the absence of a toe pinch response and normal respiration (between ~60–80 breaths per minute).

2.1.2.2 After a 2 min period of stabilization, gently rest the DCS sensor over the right hemisphere such that the top edge of the optical sensor lines up with the back of the eye and the side of the sensor lines up along the midline (Fig. 3). Cup your hand over the sensor to shield from room light. Acquire 5 seconds of data (1Hz acquisition).

2.1.2.3 Reposition sensor over the left hemisphere, acquire 5 seconds of data.

2.1.2.4 Repeat 3 times/hemisphere to account for local heterogeneities under the tissue surface.

2.1.3 Recovery

2.1.3.1 Remove mouse from anesthesia and placed on a warming pad.

2.1.3.2 After the mouse regains righting reflex, it may be returned to the cage.

2.2   DCS data analysis—2.2.1 Initial quality control: Each frame of DCS data consists of a measured normalized intensity autocorrelation function, $g_2(\tau)$ (Fig. 4A), and photon count rate (kHz).

2.2.1.1 To remove data frames with significant motion artifact, discard data frames for which the mean value of the tail of the $g_2(\tau)$ curve (i.e., $g_2(\tau > 0.018s)$) is > 1.005.

2.2.1.2 To remove data frames with poor signal-to-noise ratio, discard data frames if the detected photon count rate is < 20 kHz.

2.2.2 Extract cerebral blood flow index: Using *fminsearch* in Matlab, fit each ith measured data frame ($g_{2,meas\ i}(\tau)$) for $CBF_i(i)$. We restrict fits to $g_{2,meas\ i}(\tau) > 1.05$, and find the value of CBF_i that minimizes the following cost function:

$$\chi^2 = \sum_j \left(g_{2,\,meas\ i}\!\left(\tau_j\right) - g_{2,fit}\!\left(\tau_j\right)\right)^2, \tag{1}$$

Where the sum is over all measured delay times, τ_j, and $g_{2,meas\ i}(\tau)$ is the semi-infinite homogeneous solution of the correlation diffusion equation (Fig. 4B):

$$g_{2,\,fit}(\tau) = 1 + \beta\left(\frac{\dfrac{e^{-K(\tau)r_1}}{r_1} - \dfrac{e^{-K(\tau)r_2}}{r_2}}{\dfrac{e^{-K(0)r_1}}{r_1} - \dfrac{e^{-K(0)r_2}}{r_2}}\right)^2. \tag{2}$$

Here β is a coherence factor determined by the experimental set up, $K(\tau) = \sqrt{\left(3\mu_a\mu_s' + 6\mu_s'k_0^2\tau CBF_i\right)}$, $r_1 = \sqrt{\rho^2 + z_0^2}$, $r_2 = \sqrt{\rho^2 + (z_0 + 2z_b)^2}$, $z_0 = 1/\mu_s'$, $z_b = 2(1 + R_{eff})/3\mu_s'(1 - R_{eff})$, $R_{eff} = 0.493$ for an assumed tissue index of refraction of 1.4, ρ is 6 mm, and μ_a and μ_s' are the absorption and reduced scattering coefficient of the tissue (assumed to be 0.1 and 4.1/cm, respectively[10, 26, 27]).

NOTE: Because β can vary ~10% over time, fit each data frame for β and CBF_i simultaneously.

2.2.3 Perform secondary quality control: Within each repetition (which consists of 5 data frames), discard outliers. Outliers are defined as those CBF_i values that fall outside 1.5 standard deviations of the mean CBF_i for that repetition. If more than 1 data point is identified as an outlier, discard the entire repetition.

2.2.4 Estimate average cerebral blood flow index: Estimate an average CBF_i per hemisphere by taking the mean across all data frames for all repetitions (Fig. 4C). If no significant hemispheric differences are observed, average across hemispheres to obtain an estimate of average global CBF_i.

3. Multiplexed Quantification of Cytokines and Phospho-proteins using Luminex Assays

3.1 Tissue extraction—NOTE: Quantification of brain cytokines and phospho-signaling proteins using Luminex requires tissue extraction.

3.1.1 Euthanize:

3.1.1.1 Anesthetize mouse using 4.5% isoflurane in 100% oxygen for 1–2 min.

3.1.1.2 Check for deep plane of anesthesia via lack of toe pinch response. Euthanize via decapitation.

3.1.2 Harvest tissue:

3.1.2.1 Remove the brain. Typically, we fix the left hemisphere for histology and microdissect several regions from the right hemisphere within the cortex and hippocampus (Fig. 5).

3.1.2.2 Place dissected samples in microcentrifuge tubes, flash freeze in liquid nitrogen. For analysis of freeze-sensitive proteins, it is optimal to sub-divide tissue sections prior to flash freezing to avoid later freeze-thaw.

NOTE: The protocol can be paused, and tissue samples can be stored at −80 °C until ready to lyse samples. Alternatively, samples can be lysed, then stored at −80 °C.

3.1.3 Lyse samples:

3.1.3.1 Prepare the lysis buffer by adding protease inhibitor and 2 mM phenylmethylsulfonyl fluoride to lysis buffer.

3.1.3.2 Add 150 μL of the mixed lysis buffer per approximately 3 μg of animal tissue. For reference, mouse visual cortex tissue samples are approximately 3 μg).

3.1.3.3 To homogenize the tissue, mechanically triturate the tissue by pipetting up and down ~15–20 times using 1000 μL pipette. For optimal sample trituration, a homogenizer pestle can be used.

3.1.3.4 Place the sample tubes on a rotator for 30 min at 4 °C.

3.1.3.5 Centrifuge the samples at 4 °C for 10 min at approximately $15,000 \times g$, collect the supernatant. Samples may be processed immediately or stored at −80 °C for further analysis.

> NOTE: Sample lysates prepared using this protocol are compatible with Western blot, from which the phagocyte/microglial marker Iba1 and/or the astrocyte activation marker GFAP can be analyzed to complement cytokine and phospho-protein analysis for neuroinflammation studies [11].

3.2 Multiplex immuno-assay protocol for cytokines and phospho-proteins

> NOTE: Although similar overall, there are some minor differences in the protocols for cytokine and phospho-protein kits. Differences are noted in each step. The steps to prepare samples for the Luminex assay are outlined below.

3.2.1 Preparation of reagents (day 1, same for cytokines and phospho-proteins):

3.2.1.1 Allow reagents to warm to room temperature (~30 min).

3.2.1.2 Sonicate multiplex magnetic beads bottle for 30 seconds followed by 1 min of vortexing. Ensure multiplex magnetic beads are shielded from light with aluminum foil or use provided light protective bottles.

3.2.1.3 Prepare wash buffer by mixing 0.1% Tween20 in 1xPBS or alternatively use the wash buffer provided in the kit.

3.2.2 Preparation of lysed tissue samples (day 1, same for cytokines and phospho-proteins):

3.2.2.1 If previously frozen, remove lysed tissues samples from freezer and allow to thaw on ice (~ 20 min). Centrifuge samples for 10 min at $9,167 \times g$ to remove precipitate.

3.2.2.2 Prepare 25 μL of sample at the optimal protein concentration determined by the linear range analysis (see section 3.3). To normalize total volume for all samples, dilute samples in assay buffer provided in the kit.

3.2.3 Preparation of 96 well plate (day 1, same for cytokines and phospho-proteins):

3.2.3.1 Use the 96 well plate included in the kit or one with a thin bottom, such as Brand Tech.

3.2.3.2 Add 200 μL of wash buffer (or 1X PBS, 0.1% Tween) into each well and mix on plate shaker for 10 min at 750 rpm.

3.2.3.3 Decant wash buffer and tap the plate onto a paper towel to remove residue.

3.2.4 Immunoassay procedure for Cytokines (day 1):

3.2.4.1 Add the following to each well in order:

3.2.4.1.1 25 μL assay buffer to all wells.

3.2.4.1.2 25 μL of additional assay buffer ONLY to background wells. For every experimental run, it is recommended to have at least two background wells. Background wells have no sample loaded and define the fluorescent intensity read by the instrument without sample.

3.2.4.1.3 25 μL of each diluted sample to corresponding sample wells.

3.2.4.1.4 25 μL of 1x multiplex magnetic beads to all wells (Fig. 6). Be sure to vortex beads for 1 min before adding to wells.

3.2.4.2 Seal plate with plate sealer and cover the plate with aluminum foil. Incubate overnight (12–16 hours) at 2–8 °C.

3.2.5 Immunoassay procedure for Cytokines (day 2)

3.2.5.1 Place 96 well plate on magnetic separator, making sure the wells are aligned with the magnets. Let sit for 2 min. Decant well contents while the plate is still attached to the magnetic separator.

3.2.5.2 Wash plate 2 times using the following steps:

3.2.5.2.1 Add 200 μL wash buffer, place on shaker for 2 min at room temperature.

3.2.5.2.2 Place the well plate on the magnetic separator for 2 min at room temperature.

3.2.5.2.3 Decant well contents while well plate is still attached to magnetic separator.

3.2.5.3 Add 25 μL of detection antibody per well (Fig. 6). Cover with foil. Incubate for 1 hour on plate shaker (750 rpm) at room temperature.

3.2.5.4 Leave detection antibody in and add 25 μL streptavidin-phycoerythrin (SAPE) to each well (Fig. 6). Cover with foil. Incubate for 30 min on plate shaker (750 rpm) at room temperature

3.2.5.5 Place well plate on magnetic separator, let sit for 2 min. Decant well contents, detach from magnetic separator.

3.2.5.6 Wash well plate two times (see step 3.2.5.2)

3.2.5.7 Add 75 μL Luminex Drive Fluid (if using MAGPIX instrument) or assay buffer (if using 200 or FlexMap 3D instrument) to each well. Re-suspend beads on plate shaker for 5 min at room temperature.

3.2.5.8 Read on Luminex Instrument (MAGPIX, 200, or FlexMap 3D), referring to the user's manual for proper operation (Fig. 6).

3.2.6 Immunoassay procedure for phospho-proteins (day 1):

3.2.6.2 Add the following to each well in order:

3.2.6.1.1 25 μL assay buffer to all wells

3.2.6.1.2 25 μL of additional assay buffer ONLY to background wells. For every experimental run, it is recommended to have at least two background wells. Background wells have no sample loaded and define the fluorescent intensity read by the instrument without sample.

3.2.6.1.3 25 μL of each diluted sample to each sample well.

3.2.6.1.4 25 μL of 1x multiplex magnetic beads to all wells (Fig. 6).

> NOTE: The Luminex assay kit provides multiplex magnetic bead in 20x stock solution. Be sure to vortex 20x stock multiplex magnetic bead solution for 2 min, and then dilute it in assay buffer to 1x solution. Vortex 1x multiplex magnetic bead suspension for 1 min before adding to wells.

3.2.6.2 Seal plate with plate sealer and cover the plate with aluminum foil. Incubate overnight (12–16 hours) at 2–8 °C.

3.2.7 Immunoassay procedure for phospho-proteins (day 2)

3.2.7.1 Place well plate on magnetic separator, making sure the well plate is fully aligned with the magnetic separator. Let sit for 2 min. Decant well contents while the well plate is still attached to the magnetic separator.

3.2.7.2 Wash plate 2 times (see step b in cytokine's immunoassay procedure day 2)

3.2.7.3 Dilute the 20x stock detection antibody to 1x solution in assay buffer. Add 25 μL of 1x detection antibody per well (Fig. 6). Cover with foil. Incubate for 1 hr on plate shaker (750 rpm) at room temperature.

3.2.7.4 Next, place 96 well plate on magnetic separator, let sit for 2 min. Decant well contents, detach from the magnetic separator

3.2.7.5 Dilute 25x stock SAPE in assay buffer to 1x buffer. Add 25 μL of 1x SAPE (Fig. 6). Cover with foil and incubate for 15 min on plate shaker (750 rpm) at room temperature.

3.2.7.6 Leave the SAPE in wells, and add 25 μL of amplification buffer to each well. Cover with foil. Incubate for 15 min on plate shaker (750 rpm) at room temperature.

3.2.7.7 Incubate for 15 min on plate shaker (750 rpm) at room temperature.

3.2.7.8 Place the well plate on the magnetic separator for 2 min. Decant well contents, detach from magnetic separator.

3.2.7.9 Add 75 μL Luminex Drive Fluid (if using MAGPIX instrument) or assay buffer (if using 200 or FlexMap 3D instrument). Re-suspend beads on plate shaker for 5 min at room temperature.

3.2.7.10 Read on Luminex instrument (MAGPIX, 200, or FlexMap 3D), referring to the user's manual for proper operation (Fig. 6)

3.3 Linearity of sample dilution curve—3.3.1 Preparation of samples: Serially dilute test samples with different concentration of total protein. For bulk brain tissues, load serial dilutions from 0–25 μg for cytokines and 0–12 μg for phospho-proteins. Total protein concentration can be measured using bicinchoninic acid (BCA) assay.

3.3.2 Multiplex immunoassay: Perform the Luminex assay (see section 3.2) on selected samples.

3.3.3 Data analysis:

3.3.3.1 Plot fluorescent intensity for each protein vs. amount of protein loaded (Fig. 7).

3.3.3.2 For each analyte, identify range of total protein loaded for which the relationship between total protein and the fluorescent intensity readout is linear (Fig. 7).

3.3.3.3 To determine the amount of total protein that should be loaded for the full assay run, identify the linear portion of the curve for each analyte and then select a protein concentration that falls within the linear range for the majority of analytes.

NOTE: Although most proteins share a similar linear range, the linear ranges may not overlap for all proteins. If this is the case, it may be necessary to run each sample multiple times with different amounts of total protein loaded. Alternatively, nonlinear samples may be left out of the analysis. Additionally, some proteins may not have a linear range whatsoever.

4. Partial Least Squares Regression

Note: Sample R code and a sample data spreadsheet are provided to carry out the Partial Least Squares Analysis.

4.1 Data Preparation: Format your data as shown in the provided sample data spreadsheet, "MyData". Include variable names in the row 1, sample names in column A, the response variable in column B, and all predictor variables in columns C+. Fill your last two rows with your background data, and set both sample names to "Background".

4.2 Partial Least Squares Regression in RStudio—4.2.1 Install R from www.r-project.org (free, open source).

4.2.2 Install RStudio Desktop from www.rstudio.com (free, open source license).

4.2.3 Download the sample R code provided with this publication, "PLSR_Sample_Code.R" and save it to the same folder that contains your data spreadsheet. Open the code file in RStudio.

4.2.4 In the "User Input" section, change "dataFileName" to the name of your data spreadsheet.

4.2.5 Carry out the following steps by highlighting the section of code you wish to run and clicking "Run" in the top right corner of your script.

4.2.5.1 Load necessary R packages, functions, the working directory address, and user input values in RStudio (subsection "Preliminaries").

4.2.5.2 Load your data into RStudio and prepare raw data for processing by subtracting mean background signal from all measurements and z-scoring each analyte (subsection "Read Data and Subtract Background")(Fig. 8A).

4.2.5.3 Perform partial least squares regression in RStudio using the plsRglm package v1.2.5[28] available on the Comprehensive R Archive Network (CRAN). Perform a varimax rotation (stats package v3.6.2)[23] in the LV1-LV2 plane to identify a new horizontal axis that best separate samples by the response variable (subsection "PLS")(Fig. 8B).

4.2.5.4 Conduct a Leave One Out Cross Validation (LOOCV) in which one sample is iteratively left out of the data and the PLSR model is re-computed. Compute standard deviation for analyte loadings across all LOOCV runs (subsection "LOOCV").

4.3   Create Representative Plots: Run the provided sample code as detailed above to create representative plots which automatically export as pdf files to your working directory (the folder containing your data and code files).

4.3.1 Create a heat map of the processed data as shown in Fig. 8A (subsection "PLS"). Color each entry along a spectrum defined by z-score. Sort analytes by the order computed in the latent variable of interest.

4.3.2 Create a scores plot with LV1 scores plotted along the horizontal axis and LV2 scores plotted along the vertical axis, as shown in Fig. 8B (subsection "PLS"). Color each data point according to its response variable measurement to visualize the relationship between each latent variable and the response variable.

4.3.3 Create a bar plot displaying loadings for each of your predictor variables to visualize how each analyte contributes to the latent variables, as shown in Fig. 8C (subsection "LOOCV").

4.3.4 Create a plot regressing LV1 scores against your response variable to visualize how well the PLSR model separates the samples, as shown in Fig. 8D (subsection "PLS").

REPRESENTATIVE RESULTS

Previously collected data were taken from our prior work in which a group of eight C57BL/6 mice were subjected to three closed-head injuries (Fig. 2) spaced once daily[11]. In this work, cerebral blood flow was measured with Diffuse Correlation Spectroscopy 4 hr after the last injury (Fig. 3,4). After post-injury CBF assessment, the animals were euthanized and brain tissue was extracted for quantification of cytokines and phospho-proteins via immunoassay (Fig. 5). We also quantified the phagocyte/microglial activation marker Iba1 via Western blot (methods described in[11]). Brain tissue from each mouse was lysed, and total protein

concentration was measured using a BCA assay. Multiplexed cytokine quantification was conducted using the Milliplex MAP Mouse Cytokine/Chemokine 32-Plex, which was read using a Luminex MAGPIX system (Fig. 6). A linear range analysis was conducted to determine an appropriate protein loading (12 μg of protein per 12.5 μL of lysate) (Fig. 7) prior to collecting data from all samples.

Cytokine data was prepared for analysis by subtracting background measurements from sample data, then z-scoring data for each analyte (Fig. 8A). A heatmap was generated from z-scored data to visualize differences in cytokine expression among animals. Partial Least Squares Regression (PLSR) was conducted using the phagocyte/microglial activation marker Iba1 as the response variable and cytokine measurements as the predictor variables (Fig. 8B). A varimax rotation was performed to maximize the co-variance of the data on LV1 with the Iba1 measurements (Fig. 8D). High loading weights in LV1 (Fig. 8C) correspond with the cytokine expression most associated with high expression of Iba1. Linear regressions between Iba1 and cytokines show that those cytokines with the greatest loading weights in LV1 were also statistically significant (Fig. 8E).

DISCUSSION

Herein we detail methods for assessment of the hemodynamic and neuroinflammatory response to repetitive mild traumatic brain injury. Further, we have shown how to integrate these data as part of a multivariate systems analysis using partial least squares regression. In the text below we will discuss some of the key steps and limitations associated with our protocol as well as the advantages/disadvantages of our methods over existing methods:

Weight-drop model of mild traumatic brain injury:

This method of traumatic brain injury induction is advantageous in that it features blunt-impact followed by rapid anterior-posterior rotational acceleration commonly seen in sports-related head injuries[10, 19]. Certainly, the lissencephalic mouse brain does not fully recapitulate complexity of the gyrocephalic human brain; nevertheless, this model does induce many of the same clinical and behavioral sequelae of human mTBI, including sustained deficits in spatial learning and memory with repeated injuries. Additionally, while the impact is mild in nature (no structural/neuronal damage, no blood brain barrier permeability, cognitive deficits emerging only after multiple hits, etc.[19]), it does induce significant loss of consciousness, in contrast to humans where loss of consciousness is less common. This increased loss of consciousness may be due to an interaction with the anesthesia given immediately prior to the impact, although the exact cause is not well understood. Finally, we note that aligning the guide tube such that the bolt impacts between the coronal and lamdoid sutures is critical. We have observed that impacts that are more posterior can cause significant motor deficits that require euthanasia.

Assessment of cerebral blood flow with Diffuse Correlation Spectroscopy:

Non-invasive, longitudinal measurements of cerebral blood flow (CBF) with traditional modalities used in human/large animal studies, such as perfusion magnetic resonance imaging or transcranial Doppler ultrasound, are challenging in mice for various reasons,

including small brain size and total blood volume[29]. Diffuse Correlation Spectroscopy is well-suited in mice and offers the added advantages of being noninvasive and relatively inexpensive compared to other modalities[20, 30]. Because DCS is sensitive to motion artifacts, mice need to be briefly anesthetized or restrained for assessment. We typically use isoflurane anesthesia due to its fast induction and recovery; however, isoflurane is a cerebral vasodilator, and blood flow estimates under isoflurane should be interpreted with caution. Decreases in blood flow seen post-injury compared with sham-injured animals could be confounded by a failure of the injured cerebral vasculature to vasodilate in response to isoflurane. Finally, we have previously demonstrated excellent intra-user repeatability of blood flow measurements with DCS in mice but only fair intra-user repeatability [21]. For this reason, we recommend that the same operator acquire DCS measurements for experiments that require longitudinal assessment of cerebral blood flow.

Multiplexed quantification of cytokines and phospho-proteins using Luminex assays:

A key challenge with any ELISA is the Hook effect, whereby increased protein concentration can reduce antibody affinity for the target protein, thus leading to decreased assay signal in response to increased protein[31] (Fig. 7). This effect can be exacerbated when analyzing whole tissues, wherein bulk proteins can similarly interfere. Thus, the first step in utilizing Luminex assays is to determine if there is a range of protein concentrations loaded for which the assay read out linearly varies with the amount of protein loaded. Analytes that do not have such a linear range (Fig. 7) should be excluded from analysis. We also note that cytokine levels in the brain are typically very low and appear near the lower detection limit assessed via standard curves supplied with the Luminex kit. For this reason, it is essential to conduct linear ranging analysis to determine if the instrument readout truly reflects the amount of sample loaded. For key proteins of interest, this linear range analysis can be complemented with a spike recovery assay wherein recombinant protein is spiked into a sample, and linearity in the instrument reading is evaluated[32].

Because neuroinflammation is regulated by diverse intracellular phospho-proteins and extracellular cytokines, it is critical to simultaneously measure a wide array of these proteins in order to understand the brain's neural immune response to mTBI. Luminex multiplexed immunoassays enable simultaneous quantification of dozens of cytokines and phospho-proteins from a single sample, providing a holistic view of the tissue immune response post-injury. Although these analyses provide a broad view of cytokines/chemokines as well as phospho-proteins, the assay quantifies total amount of each protein from a tissue homogenate. Thus, it does not yield cell-type specific data. Cell-type specificity can be determined by follow-up immunohistochemistry to identify localization of top proteins of interest with markers for cell types (e.g., neurons, microglia, astrocytes, etc.)[11].

Partial least squares regression analysis for data integration:

The tissue response to mTBI is multifactorial, consisting of physiological changes in blood flow together with changes in the phagocyte/microglial activation marker Iba1, diverse cytokines, and phospho-proteins, among others[11]. Because of the multiplexed nature of the data collected, a systematic method is needed to account for the multidimensionality of the relationships between the various predictor variables. PLSR provides a suitable

solution to this problem by identifying LVs that maximally identify the co-variance between the predictor variables and the outcome variable (e.g., Iba1 in Fig. 8). Importantly, those proteins found to strongly correlate with the predictor variable (i.e., those with high loadings on LV1) often correlate in the univariate regression analysis as well (Fig. 8E). Because PLSR is often used to fit a large number of predictor variables to a smaller number of samples as in Fig. 8, it is critical to gain an understanding of the sensitivity of the weights on LV1 to individual samples. For a small number of samples (<10) LOOCV is useful for assessing the sensitivity of the weights (indicated via SD error bars in Fig. 8C). For a larger number of samples, it will be important to assess sensitivity by leaving multiple samples out at a time using a Monte Carlo sub-sampling approach[33]. We refer the reader to *Multi and Megavariate Data Analysis* [24] for an in-depth discussion of PLSR approaches and uses. Finally, we note that a key limitation of this type of analysis is that it is purely correlative. PLSR does not prove a mechanistic relationship between predictor variables and the outcome variable. We view PLSR as a valuable *hypothesis generating* approach that is used to suggest tractable targets to modulate in future experiments that establish causal relationships.

Supplementary Material

Refer to Web version on PubMed Central for supplementary material.

ACKNOWLEDGMENTS:

REFERENCES

1. Langlois JA, Rutland-Brown W, Wald MM The epidemiology and impact of traumatic brain injury: a brief overview. J Head Trauma Rehabil. 21 (5), 375–8 (2006). [PubMed: 16983222]

2. Iraji A et al. Resting State Functional Connectivity in Mild Traumatic Brain Injury at the Acute Stage: Independent Component and Seed-Based Analyses. J Neurotrauma. 32 (14), 1031–45, doi: 10.1089/neu.2014.3610 (2015). [PubMed: 25285363]

3. Guskiewicz KM et al. Cumulative effects associated with recurrent concussion in collegiate football players: the NCAA Concussion Study. Jama. 290 (19), 2549–55 (2003). [PubMed: 14625331]

4. Longhi L et al. Temporal window of vulnerability to repetitive experimental concussive brain injury. Neurosurgery. 56 (2), 364–74 (2005). [PubMed: 15670384]

5. Committee on Sports-Related Concussions in Youth, Board on Children, Youth, and Families, Institute of Medicine, National Research Council Sports-Related Concussions in Youth: Improving the Science, Changing the Culture. at <http://www.ncbi.nlm.nih.gov/books/NBK169016/>. National Academies Press (US). Washington (DC). (2014).

6. Barkhoudarian G, Hovda DA, Giza CC The Molecular Pathophysiology of Concussive Brain Injury - an Update. Phys Med Rehabil Clin N Am. 27 (2), 373–93, doi: 10.1016/j.pmr.2016.01.003 (2016). [PubMed: 27154851]

7. McCrory P et al. Consensus statement on concussion in sport--the 4th International Conference on Concussion in Sport held in Zurich, November 2012. Clin J Sport Med. 23 (2), 89–117, doi: 10.1097/JSM.0b013e31828b67cf (2013). [PubMed: 23478784]

8. Belanger HG, Vanderploeg RD, Curtiss G, Warden DL Recent neuroimaging techniques in mild traumatic brain injury. J Neuropsychiatry Clin Neurosci. 19 (1), 5–20, doi: 10.1176/appi.neuropsych.19.1.5 (2007). [PubMed: 17308222]

9. Sours C, Zhuo J, Roys S, Shanmuganathan K, Gullapalli RP Disruptions in Resting State Functional Connectivity and Cerebral Blood Flow in Mild Traumatic Brain Injury Patients. PLoS ONE. 10 (8), e0134019, doi: 10.1371/journal.pone.0134019 (2015). [PubMed: 26241476]

10. Buckley EM et al. Decreased Microvascular Cerebral Blood Flow Assessed by Diffuse Correlation Spectroscopy after Repetitive Concussions in Mice. Journal of Cerebral Blood Flow & Metabolism. 35 (12), 1995–2000, doi: 10.1038/jcbfm.2015.161 (2015). [PubMed: 26154866]

11. Sankar SB et al. Low cerebral blood flow is a non-invasive biomarker of neuroinflammation after repetitive mild traumatic brain injury. Neurobiology of Disease. 124, 544–554, doi: 10.1016/j.nbd.2018.12.018 (2019). [PubMed: 30592976]

12. Vagnozzi R et al. Temporal window of metabolic brain vulnerability to concussions: mitochondrial-related impairment--part I. Neurosurgery. 61, 379–88; discussion 388–9, doi: 10.1227/01.neu.0000280002.41696.d8 (2007).

13. Longhi L et al. Temporal window of vulnerability to repetitive experimental concussive brain injury. Neurosurgery. 56, 364–74 (2005). [PubMed: 15670384]

14. Fujita M, Wei EP, Povlishock JT Intensity- and interval-specific repetitive traumatic brain injury can evoke both axonal and microvascular damage. J Neurotrauma. 29, 2172–80, doi: 10.1089/neu.2012.2357 (2012). [PubMed: 22559115]

15. Angoa-Perez M, Kane MJ, Briggs DI, Herrera-Mundo N, Viano DC, Kuhn DM Animal models of sports-related head injury: bridging the gap between preclinical research and clinical reality. J Neurochem. 129, 916–31, doi: 10.1111/jnc.12690 (2014). [PubMed: 24673291]

16. Prins ML, Hales A, Reger M, Giza CC, Hovda DA Repeat traumatic brain injury in the juvenile rat is associated with increased axonal injury and cognitive impairments. Developmental Neuroscience. 32, 510–8, doi: 10.1159/000316800 (2010). [PubMed: 20829578]

17. Viano DC, Hamberger A, Bolouri H, Saljo A Concussion in professional football: animal model of brain injury--part 15. Neurosurgery. 64, 1162–73; discussion 1173, doi: 10.1227/01.neu.0000345863.99099.c7 (2009). [PubMed: 19487897]

18. Kane MJ, Angoa-Perez M, Briggs DI, Viano DC, Kreipke CW, Kuhn DM A mouse model of human repetitive mild traumatic brain injury. J Neurosci Methods. 203, 41–9, doi: 10.1016/j.jneumeth.2011.09.003 (2012). [PubMed: 21930157]

19. Meehan WP, Zhang J, Mannix R, Whalen MJ Increasing Recovery Time Between Injuries Improves Cognitive Outcome After Repetitive Mild Concussive Brain Injuries in Mice: Neurosurgery. 71 (4), 885–892, doi: 10.1227/NEU.0b013e318265a439 (2012). [PubMed: 22743360]

20. Durduran T, Yodh AG Diffuse correlation spectroscopy for non-invasive, micro-vascular cerebral blood flow measurement. NeuroImage. 85, 51–63, doi: 10.1016/j.neuroimage.2013.06.017 (2014). [PubMed: 23770408]

21. Sathialingam E et al. Small separation diffuse correlation spectroscopy for measurement of cerebral blood flow in rodents. Biomedical Optics Express. 9 (11), 5719, doi: 10.1364/BOE.9.005719 (2018). [PubMed: 30460158]

22. Lee SY et al. Noninvasive optical assessment of resting-state cerebral blood flow in children with sickle cell disease. Neurophotonics. 6 (03), 1, doi: 10.1117/1.NPh.6.3.035006 (2019).

23. Wang H, Liu Q, Tu Y Interpretation of partial least-squares regression models with VARIMAX rotation. Partial Least Squares. 48 (1), 207–219, doi: 10.1016/j.csda.2003.12.005 (2005).

24. Eriksson L, Byrne T, Johansson E, Trygg J, Vikström C Multi- and Megavariate Data Analysis Basic Principles and Applications. Umetrics Academy. (2013).

25. Conzen PF, Vollmar B, Habazettl H, Frink EJ, Peter K, Messmer K Systemic and regional hemodynamics of isoflurane and sevoflurane in rats. Anesthesia and Analgesia. 74 (1), 79–88, doi: 10.1213/00000539-199201000-00014 (1992). [PubMed: 1734802]

26. Durduran T, Choe R, Baker WB, Yodh AG Diffuse optics for tissue monitoring and tomography. Reports on Progress in Physics. 73 (7), 076701, doi: 10.1088/0034-4885/73/7/076701 (2010). [PubMed: 26120204]

27. Lee SY, Zheng C, Brothers R, Buckley EM, Buckley EM, Buckley EM Small separation frequency-domain near-infrared spectroscopy for the recovery of tissue optical properties at millimeter depths. Biomedical Optics Express. 10 (10), 5362–5377 (2019). [PubMed: 31646051]

28. Bertrand F, Maumy-Bertrand M plsRglm: Partial Least Squares Regression for Generalized Linear Models. at <https://CRAN.R-project.org/package=plsRglm>. (2019).

29. White BR, Bauer AQ, Snyder AZ, Schlaggar BL, Lee JM, Culver JP Imaging of functional connectivity in the mouse brain. PLoS One. 6, e16322, doi: 10.1371/journal.pone.0016322 (2011). [PubMed: 21283729]

30. Buckley EM, Parthasarathy AB, Grant PE, Yodh AG, Franceschini MA Diffuse correlation spectroscopy for measurement of cerebral blood flow: future prospects. Neurophotonics. 1 (1), 011009, doi: 10.1117/1.NPh.1.1.011009 (2014). [PubMed: 25593978]

31. Tate J, Ward G Interferences in immunoassay. The Clinical Biochemist. Reviews. 25 (2), 105–120 (2004). [PubMed: 18458713]

32. Staples E, Ingram RJM, Atherton JC, Robinson K Optimising the quantification of cytokines present at low concentrations in small human mucosal tissue samples using Luminex assays. Journal of Immunological Methods. 394 (1–2), 1–9, doi: 10.1016/j.jim.2013.04.009 (2013). [PubMed: 23644159]

33. Gierut JJ et al. Network-level effects of kinase inhibitors modulate TNF-α-induced apoptosis in the intestinal epithelium. Science Signaling. 8 (407), ra129, doi: 10.1126/scisignal.aac7235 (2015). [PubMed: 26671150]
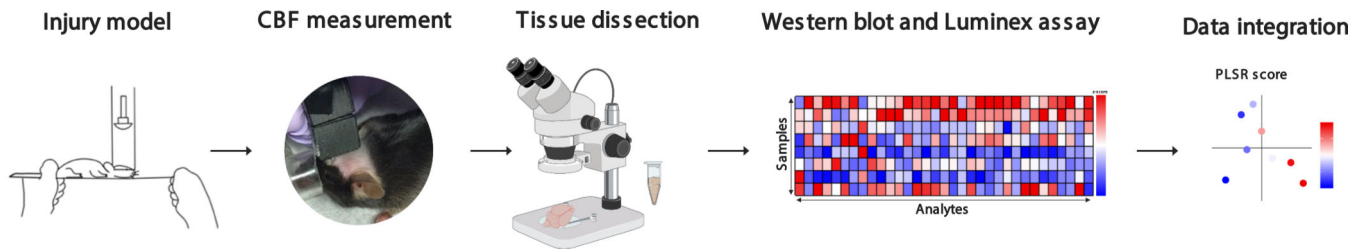
Figure 1: Typical workflow.
First, mice undergo a weight drop closed head injury, then cerebral blood flow (CBF) is measured using Diffuse Correlation Spectroscopy. Next, brains are collected, regions of interest are micro-dissected and snap frozen using liquid nitrogen. In preparation for the Luminex immunoassay, proteins are lysed, and total protein concentration is measured by BCA assay. Lysates are used for Western blot of proteins of interest and Luminex assays for cytokines and phospho-proteins. Data from CBF, Western blot, and Luminex are integrated using partial least squares regression (PLSR).
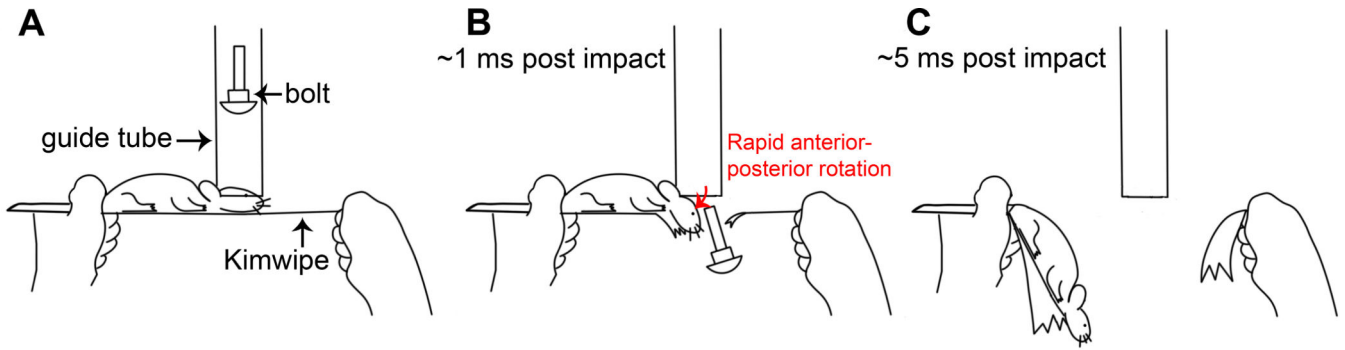
Figure 2: Closed-head weight drop model of mild traumatic brain injury.
(**A**) The anesthetized mouse is grasped by the tail and placed on a taut sacrificial membrane (KimWipe) underneath a guide tube. A 54 g weight is dropped from 1 m onto the dorsal aspect of the head. (**B**) Within ~1 ms post-impact, the mouse's head has rapidly rotated about the neck as it breaks through the sacrificial membrane. (**C**) Within ~5 ms post-impact, the entire mouse has fallen and is hanging by its grasped tail.
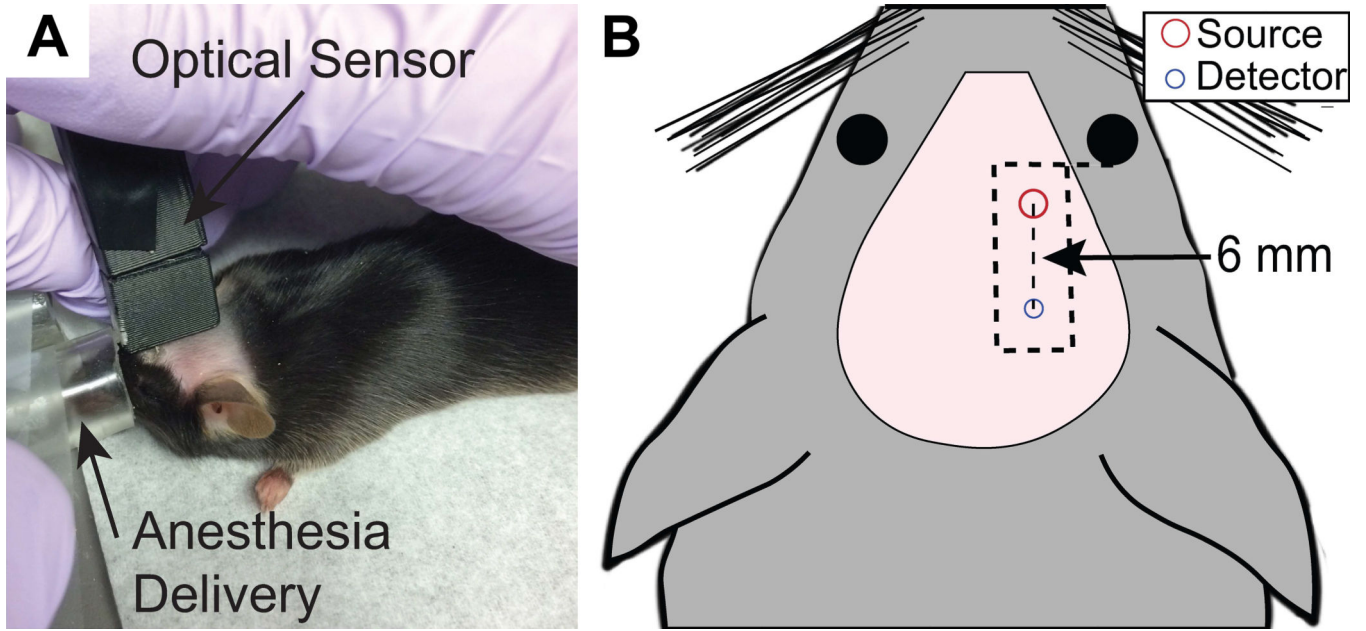
Figure 3: Measurement of cerebral blood flow by Diffuse Correlation Spectroscopy.
(**A**) An optical sensor is gently manually held over the right hemisphere to measure blood flow in an anesthetized mouse. (**B**) Representative sensor placement on the right hemisphere. The outline of the sensor is represented as a dashed black rectangle, and the location of the source and detector fibers are in red and blue circles, respectively. The sensor is placed such that the short edge of the sensor lines up with the back of the eye and the long edge of the sensor aligns with the midline.
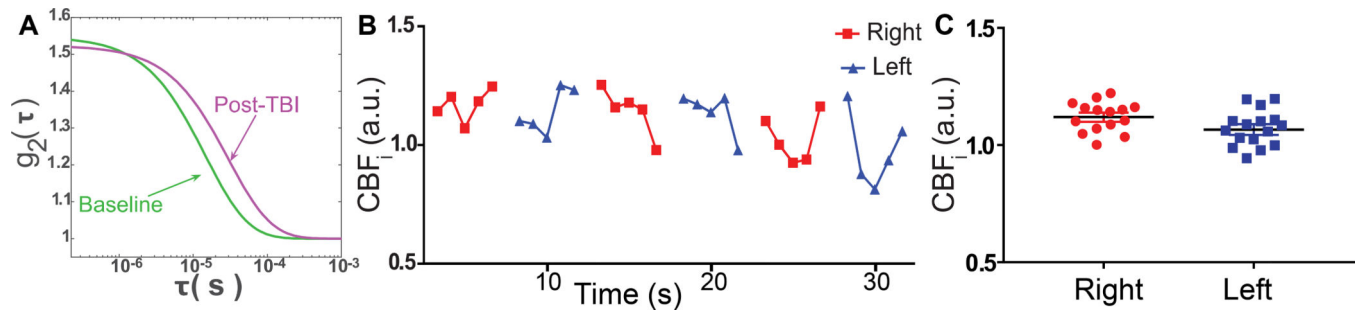
Figure 4: Diffuse Correlation Spectroscopy data analysis.
(**A**) Representative measured intensity autocorrelation curves, $g_2(\tau)$, at baseline, pre-injury baseline (green) and 4 h after 5 closed head injuries spaced once daily (purple). The right shift in the curve from pre- to post-injury reflects a decrease in blood flow. (**B**) $g_2(\tau)$ data is acquired at 1 Hz for 5 s per hemisphere and repeated 3x/hemisphere. Each measured $g_2(\tau)$ curve is fit to the semi-infinite solution to the correlation diffusion equation for a cerebral blood flow index (CBF$_i$). (**C**) CBF$_i$ values across all frames and repetitions are averaged to obtain mean cerebral blood flow index for each hemisphere.
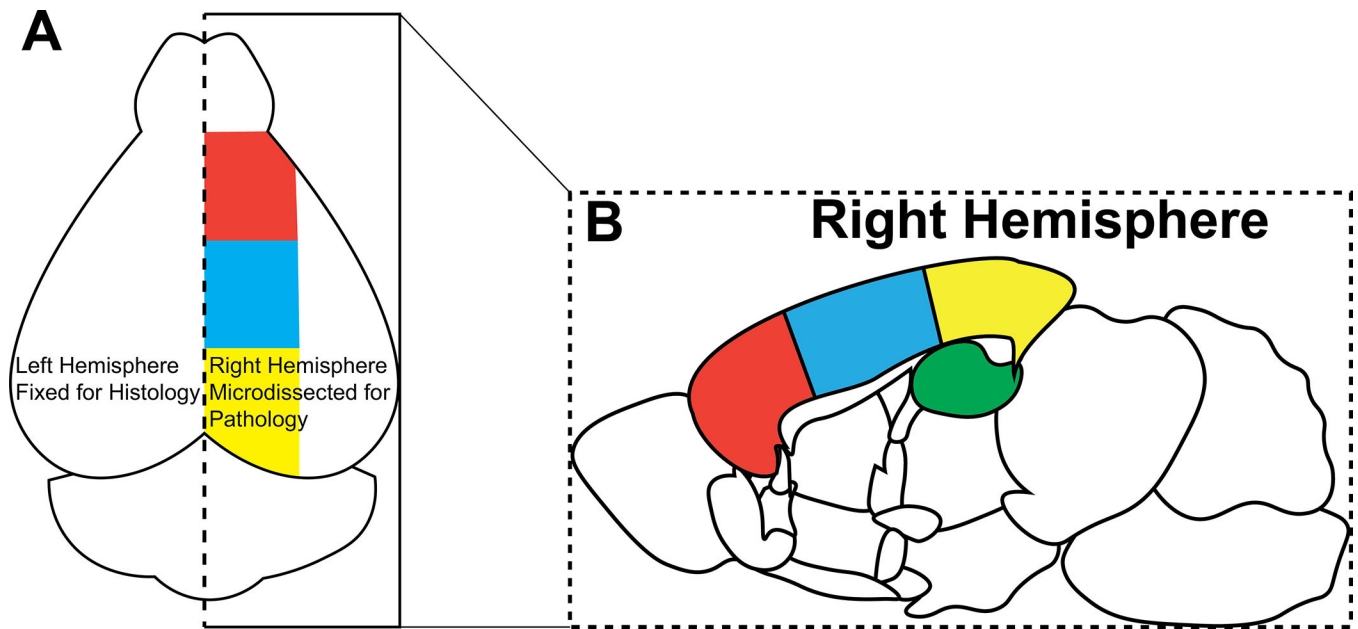
Figure 5: Mouse brain microdissection.

(**A**) After the brain is extracted from mouse, it is bisected the along dashed line. The left hemisphere is fixed for histology, and the right hemisphere is microdissected for pathology. (**B**) Sagittal view of the cortex of the right hemisphere. The right hemisphere is microdissected into corresponding color-coded regions. For analysis of freeze-sensitive proteins, it is optimal to sub-divide tissue sections prior to flash freezing.
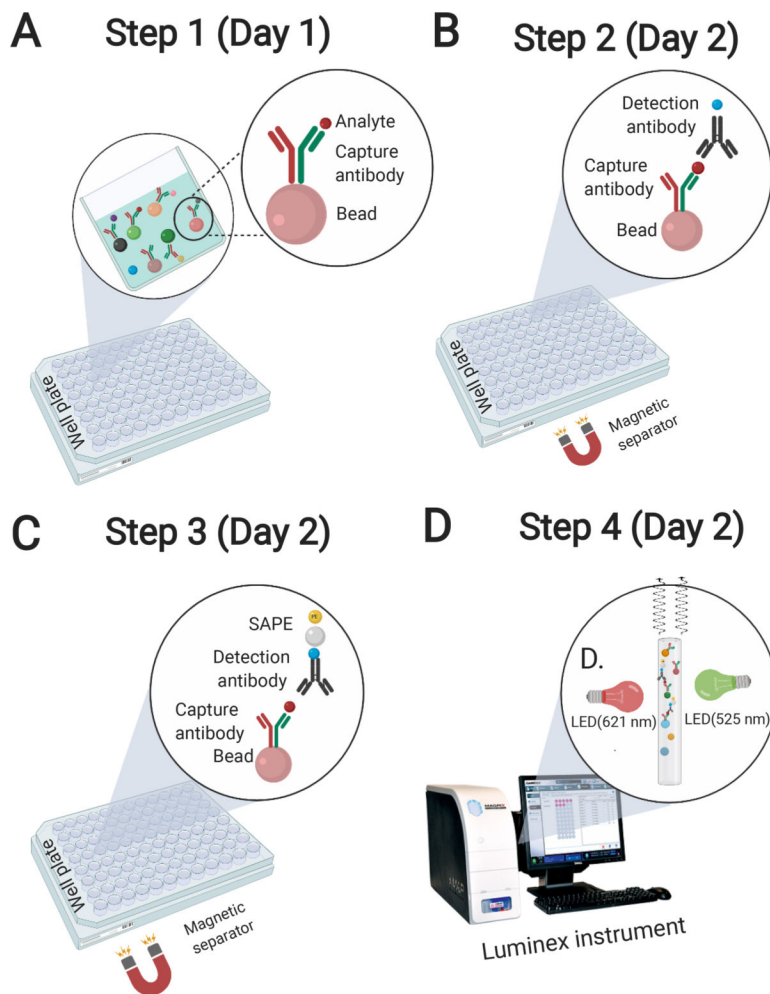
Figure 6. Illustration of Luminex procedure.
(**A**) Add samples to fluorescently tagged beads. Beads are pre-coated with a specific capture antibody for each protein of interest. (**B**) Add biotinylated detection antibodies. Biotin-detection antibodies bind to the analytes of interest and form an antibody-antigen sandwich. (**C**) Add phycoerythrin (PE)-conjugated streptavidin (SAPE). SAPE binds to the biotinylated detection antibodies, completing the reaction. For phospho-proteins, an amplification buffer (only for phospho-protein assays) is added following the addition to SAPE to enhance the assay signal. (**D**) Luminex instrument (MAGPIX, 200, or FlexMap 3D) reads reaction on each fluorescently tagged bead via a combination of red/green illumination.
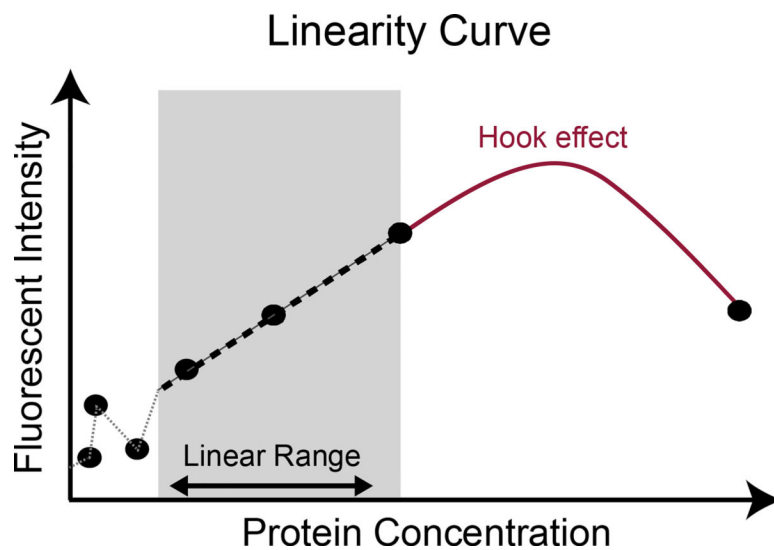
Figure 7: Illustration of sample dilution curve to identify the linear range.
Protein concentration of serially diluted samples versus fluorescent intensity measured from the Luminex assay. The linear range is defined as the protein concentration range for which the relationship between the protein concentration and fluorescent intensity is linear (arrow). In some analytes, increasing the protein concentration beyond a certain limit can decrease antibody binding such that the dilution curve becomes non-linear or inverted (Hook effect).
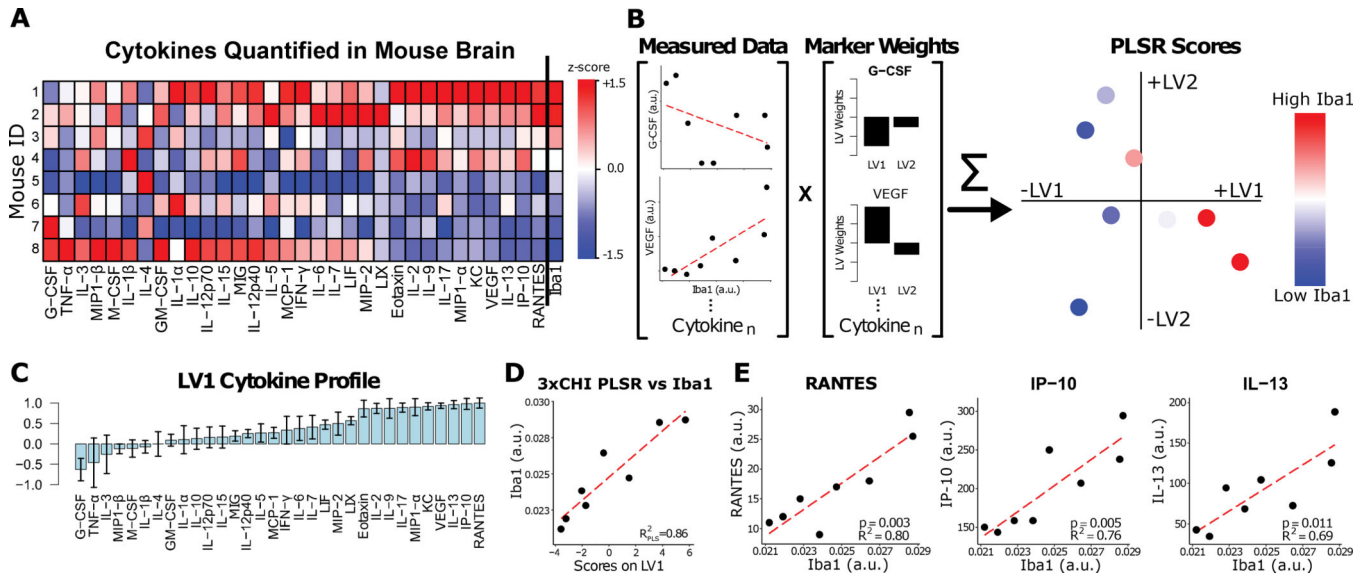
Figure 8: Representative Partial Least Squares Regression (PLSR) Analysis.
(**A**) Panel cytokine protein expression (left columns) together with Iba1 expression (righthand column) in 3xCHI mice (n=8, z-scored). (**B**) PLSR assigns weights (loadings) to measured cytokines for each latent variable. Weights are applied to measured data to compute scores for each sample on each latent variable. (**C**) PLSR of 3xCHI samples against Iba1 identified a weighted profile of cytokines, LV1, which distinguished samples by Iba1. Cytokines with negative weights were upregulated in samples with low Iba1 while cytokines with positive weights were upregulated in samples with high Iba1 (mean ± SD using a LOOCV). (**D**) Linear regression of LV1 scores for each sample against Iba1. R^2_{PLS} measures the goodness of fit between Iba1 and LV1. (**E**) Individual regressions of Iba1 against each of the cytokines with the greatest weights in LV1 in **C**.

Table of Materials

Name of Material/ Equipment	Company	Catalog Number	Comments/ Description
MILLIPLEX MAP Mouse Cytokine/Chemokine Magnetic Bead Panel - Premixed 32 Plex - Immunology Multiplex Assay	Millipore Sigma	MCYTMAG-70K-PX32	
MILLIPLEX MAPL/SAPL Signaling 10-Plex Kit-Cell Signaling Multiplex Assay	Millipore Sigma	48–660MAG	
Bio-Plex cell lysis kit	C Bio-Rad	171304012	
Luminex sheath fluid	EMD Millipore	SHEATHFLUID	
Luminex Drive Fluid	Luminex	MPXDF-4PK	
BRAND BRANDplates pureGrade Microplates, Nonsterile	BrandTech	781602 96	
Tween20	Sigma-Aldrich	P9416–50ML	
Phosphate-buffered Saline (PBS)	VWR	97064–158	
DiH2O	VWR	VWRL0200–1000	
Plate Sealer	VWR	82050–992	
Aluminum foil	VWR	89107–726	
Reagent Reservoirs	VWR	89094–668	
Polypropylene microfuge tubes	VWR	20901–547	
Phenylmethylsulfonyl fluoride	Sigma-Aldrich	P7626–1G	
Complete mini protease inhibitor tablet	Sigma-Aldrich	11836153001	
Laboratory vortex mixer	VWR	10153–838	
Adjustable pipettes			
Sonicator			
Titer plate shaker	VWR	12620–926	
Mini LabRoller rotator	VWR	10136–084	
Luminex 200, HTS, FLEXMAP 3D, or MAGPIX with xPONENT software	Luminex Corporation		
Handheld magnetic separator block for 96 well flat bottom plates	Millipore Sigma Catalogue	40–285	
1 m acrylic guide tube	McMaster-Carr	49035K85	
54 g bolt	Ace Hardware		0.95 cm basic body diameter, 2 cm head diameter, 10.2 cm length
Isoflurane 250 mL	MED-VET INTERNATIONAL	RXISO-250	
Kimwipe (11.2 x 21.3 cm)	VWR	21905–026	
852 nm long-coherence length laser	TOPTICA Photonics	iBeam smart	
4 photon counting avalanche photodiode	Perkin-Elmer	SPCM-AQ4C-IO	
Hardware Autocorrelator Board	www.correlator.com	Flex05–8ch	
LabView	National Instruments	LabVIEW	
400 um multimode source fiber	Thorlabs Inc.	FT-400-EMT	
780 nm single mode detector fiber	Thorlabs Inc.	780HP	
Depilatory cream	Amazon	Nair	